agronomy

MDPI

Article

Deterministic Process Dominated Belowground Community Assembly When Suffering Tomato Bacterial Wilt Disease

Hong Liu [1,2], Feifei Sun [3], Junwei Peng [1,2], Minchong Shen [1], Jiangang Li [1,2,*] and Yuanhua Dong [1,2]

[1] CAS Key Laboratory of Soil Environment and Pollution Remediation, Institute of Soil Science, Chinese Academy of Sciences, Nanjing 210008, China; liuhong@issas.ac.cn (H.L.); pengjw@issas.ac.cn (J.P.); mcshen1124@163.com (M.S.); yhdong@issas.ac.cn (Y.D.)
[2] University of Chinese Academy of Sciences, Beijing 100049, China
[3] Nanjing Agricultural Technique Extension Station, Nanjing 210036, China; ffsun_2044@163.com
* Correspondence: jgli@issas.ac.cn; Tel.: +86-25-86881370

Abstract: Soil microbial communities are closely associated with ecosystem functions. However, unravelling the complex nature of the microbial world and successfully utilizing all positive interactions for multipurpose environmental benefits is still a major challenge. Here, we describe the soil bacterial communities in different niches of healthy and diseased tomatoes under natural conditions. A higher abundance of the pathogen *Ralstonia solanacearum* and lower bacterial diversity were observed in the disease samples. The healthy tomato rhizosphere harbored more plant-beneficial microbes, including *Bacillus* and *Streptomyces*. Also, the co-occurrence network in the healthy rhizosphere samples was more complicated, so as to better adapt to the soil-borne pathogen invasion. Both the beta nearest-taxon-index (βNTI) and normalized stochasticity ratio (NST) analyses demonstrated that healthy rhizosphere communities were less phylogenetically clustered and mainly dominated by dispersal limitation, while homogeneous selection was the major assembly process driving the rhizosphere community of diseased samples. The results obtained with community assembly methods and co-occurrence network analysis revealed that healthy rhizosphere bacterial communities possessed potentially broader environmental stress (soil-borne pathogen stress) adaptability compared with diseased rhizosphere bacterial communities. In conclusion, this study contributed to widening our understanding of the potential mechanisms of soil bacterial community composition and assembly responding to soil-borne pathogen invasion.

Keywords: bacterial community; beneficial microbes; community assembly; co-occurrence network; *Ralstonia solanacearum Y*

Citation: Liu, H.; Sun, F.; Peng, J.; Shen, M.; Li, J.; Dong, Y. Deterministic Process Dominated Belowground Community Assembly When Suffering Tomato Bacterial Wilt Disease. *Agronomy* **2022**, *12*, 1024. https://doi.org/10.3390/agronomy12051024

Academic Editors: Richard Allen White III and Kiwamu Tanaka

Received: 30 January 2022
Accepted: 11 April 2022
Published: 24 April 2022

1. Introduction

Intensive cropping systems, characterized by continuous monoculture and intensive cultivation practices, are widespread in China, and their increased adoption has led to the outbreak of soil-borne diseases and other environmental problems, including poor soil quality and nutrient imbalances [1]. Continuous monoculture enriches soil-borne pathogenic microorganisms, which, in turn, disrupt microbial ecological balance [2]. Soil-borne pathogens infect crops and cause massive economic losses [3,4], and pose major threats to sustainable agricultural development and production. Consequently, understanding the underlying factors driving plant pathogen infection under intensive cropping systems is essential for ensuring high crop yield and quality, in addition to future food security.

It was estimated that each gram of soil, especially in the case of rhizosphere soils surrounding plant roots, harbor billions of microorganisms, and soil microbes participate in keeping the soil healthy and inhibit soil-borne diseases within agroecosystems [5]. A previous study demonstrated that soil health was maintained by interactions among microbial communities, host plants, and environmental factors [6]. In addition, rhizosphere microbial communities participated in soil nutrient cycling, abiotic factor stress

tolerance, and pathogen invasion resistance [7–9], and they could serve as an important line to defend against soil-borne diseases [10,11]. Rhizospheres are usually considered to be biological hotspots and their microbial community structures differ from that of the bulk soil [12]. In addition, bacterial community composition could vary significantly under different niches (rhizosphere soil and bulk soil), with bacterial diversity increasing with an increase in distance from the soil to the roots [13]. Microbial diversity may act as a shield against pathogen invasion, and this effect was often attributed to competition for limited resources [14,15], as a more diverse microbial community may be beneficial to make the most of available resources, while limiting the living space and nutrient resources of the pathogen [16]. Soil microorganisms engage in a higher diversity of microbial community so as to shape complicated community networks which may influence plant health [17]. Also, the microbial community composition, diversity, and interaction network is closely related to invasion of the soil-borne pathogen *Ralstonia solanacearum* [15]. Once infected by the soil borne pathogen, host plants act quickly and change their community composition via recruiting some beneficial microbes, such as *Bacillus* and *Streptomyces*, or directly repelling the pathogen by activating their immune system [18]. At the same time, alongside biotic factors, abiotic factors also have some effect, and it has been demonstrated that available nutrients may strengthen the resistance to pathogen invasion via resource competition [19], and thus regulate competition between the soil-borne pathogen and beneficial microbes. In addition, recent studies have demonstrated that microbial community structure development processes involve stochastic processes [20,21]. However, at present, most studies about plant disease have focused more on taxonomic diversity, patterns of community structure, and function, and few studies have focused their attention on discussion of the relationship between the microbial community assembly process and plant disease, so that the underlying mechanisms driving such community assembly patterns remain unclear.

Community assembly has increasingly been considered one of the approaches to studying microbial community structure [22]. The microbial community is driven by both deterministic processes and stochastic processes, which are dominant in microbial communities under different environments [23,24]. When deterministic processes are dominant, selection via biotic or abiotic factors deeply influences the shaping of the microbial community [25]; conversely, when stochastic processes are dominant, microbial community structure is greatly influenced by community dispersal, that is, the microbial community is more adaptable to the influence of the external environment [26]. Thus, it was vital to assess the relative contributions of deterministic processes (homogeneous selection and variable selection) and stochastic processes (dispersal limitation, homogeneous dispersal, and undominated process) shaping microbial communities [27,28]. It had been found that upland ecosystems were dominated by deterministic processes (homogeneous selection), while flooded ecosystems were more affected by stochastic processes (homogeneous dispersal) [29]. Environmental factors (biotic and abiotic factors) usually regulate the balance of stochastic and deterministic assembly processes [20,27,30,31], and a balanced stochastic and deterministic assembly process is beneficial to maintain a diverse ecosystem [29]. Changes in soil moisture content, and organic matter content, alter the relative effects of different assembly processes in dominating soil bacterial communities [20,27]. Moreover, extreme environmental factors, such as extreme soil salinity and pH, could drive the deterministic assembly of soil bacterial communities, and suitable soil pH values and less salinity content could contribute to the stochastic in the process of soil generation [30,31]. Thus, it is easily speculated that there may be a transformation between environment factors and community assembly. At present, there is much research on the effect of non-biological factors on the assembly of microbial communities, but it is not clear whether, and how, biological factors, such as soil-borne pathogens, mediate deterministic or stochastic assembly processes in bacterial community assembly. Understanding the types of assembly processes driving microbial community structure under soil borne pathogen infection remains a crucial challenge for understanding the occurrence of soil-borne diseases. The βNTI (beta nearest-taxon-index) and NST (normalized stochasticity ratio) are currently

two main community assembly methods [32,33]. The application of various microbial community assembly methods to soil-borne disease might be beneficial to help understand the occurrence of plant soil-borne diseases.

Plant bacterial wilt disease (BWD), caused by *R. solanacearum*, is a devastating plant disease, and affects a variety of plants, such as tomato, tobacco, and eggplant, with massive associated crop losses globally [34]. Bacterial wilt disease dynamics are variable and often accompanied by a change in microbial community. To further understand the relationship between the BWD infection and microbial communities in detail, we collected soil samples in different soil niches (rhizosphere soils and bulk soils) of diseased and healthy tomato plants. We planned to explore: (i) how the diversity and composition of the microbial community changed under *R. solanacearum* invasion, and (ii) how the soil microbial community assembly processes responded to the soil-borne pathogen invasion. Our research intended to confirm above conjectures through neutral model, network construction, and the community assembly methods (βNTI and NST), thereby helping to widen our understanding of the potential mechanisms of soil microbial community composition and assembly in response to soil-borne pathogen invasion.

2. Materials and Methods

2.1. Collection of Plant and Soil Samples

This experiment was carried out on a research base of vegetables and flowers in Hengxi Town, Nanjing city, Jiangsu province, China (118°46′ E, 31°43′ N). The typical soil here is yellow-brown earth (Udic Argosol). After four successive years of tomato mono-cultured with 2 seasons per year, bacterial wilt disease (BWD) occurred naturally and randomly in the field. Bacterial wilt symptoms were assessed and scored 0, 1, 2, 3, and 4, based on the degree of withering of the tomato leaves, according to our previous research [35,36]. The sample collection was carried out on 11 November 2019. A total of 12 tomato plants (including six healthy plants and six diseased plants, considering there were few completely healthy plants; here we defined healthy plants with disease grades of 0 and 1, and diseased plants were 2, 3, and 4) and their corresponding bulk soil samples, 15 cm away from roots, were collected (five subsamples were thoroughly mixed as a biological sample). The plants and soil samples were placed on pre-prepared ice and then transported to the laboratory. Generally, the root-adhering rhizosphere soil samples were collected using a brush. Consequently, a total of 24 samples, including six bulk soil samples from high BWD infected plants (BSD), six bulk soil samples from healthy plants (BSH), six rhizosphere soil samples with high BWD infected plants (RSD), six rhizosphere soil samples with healthy plants (RSH), were obtained. Finally, all treated soil samples were preserved at −80 °C for further soil DNA extraction. Each treatment contained six replicates.

2.2. Soil Physicochemical Analysis

The soil's physicochemical properties were analyzed by the method described by Lu [37]. Soil pH and electric conductivity (Ec) were detected with a pH meter and S230 m respectively (Thermo Orion-868, Waltham, MA, USA), using soil water suspension (soil: water 1:2.5 for pH and 1:5 for Ec). The potassium dichromate oxidation method was applied to measure soil organic carbon (SOC). After digesting with hydrofluoric acid (HF) and then with perchloric acid ($HClO_4$), the total nitrogen (TN) was measured with an elemental analyzer (Vario MAX, Elementar, Germany). Soil NO_3^--N and NH_4^+-H were extracted with 2 M KCl solution (1:5 w/v), and then detected with continuous flow analyzer (San++, Skalar Analytical B.V., Breda, The Netherlands). The flame photometry (FP640, INASA, Shanghai, China) and the molybdenum blue method were applied to detect total potassium (TK) and total phosphorus (TP) respectively, extracting by means of ammonium acetate firstly, and available potassium (AK) was then detected by flame photometry. The available phosphorus (AP) was extracted using 0.5 M sodium bicarbonate ($NaHCO_3$) and quantified following the molybdenum blue method.

2.3. DNA Extraction, Gene Amplification and Sequencing

To extract DNA, 0.5 g soil was weighed and the Fast DNA Spin kit (MO Bio, Carlsbad, CA, USA) was employed, according to its manufacturer's instructions. The concentrations and quality of DNA were confirmed using a NanoDrop 2000 spectrophotometer (Thermo Scientific, Wilmington, DE, USA). The bacterial 16S rDNA V4–V5 regions were amplified using primers 515F (5′-GTGCCAGCMGCCGCGG-3′) and 907R (5′-CCGTCAATTCMTTTRAGTTT-3′), where the barcode was an eight-base sequence unique to each sample, using the paired barcoded primer [38]. The 20-μL PCR reaction mixtures consisted of the following components: 4-μL of 5× FastPfu buffer, 2-μL 2.5 mM dNTPs, 0.8-μL 5 μM forward primer, 0.8-μL 5 μM reverse primer, 0.4-μL FastPfu Polymerase, 0.2-μL bovine serum albumin, 1.0-μL 10 ng of template DNA, and double distilled water (ddH_2O). The PCR reaction was carried out at 95 °C for 3 min, followed by 35 cycles at 95 °C for 30 s, 55 °C for 30 s, 72 °C for 45 s, and a final extension at 72 °C for 10 min. Amplicons were extracted from 2% agarose gels and purified using the AxyPrep DNA Gel Extraction Kit (Axygen Biosciences, Union City, CA, U.S.) according to the manufacturer's instructions and quantified using QuantiFluor™ -ST (Promega, Madison, Wisconsin, USA). The purified PCR products were quantified by Qubit®3.0 (Life Invitrogen, Carlsbad, CA, USA) and every amplicon, whose barcodes were different, were mixed equally. The pooled DNA product was used to construct Illumina Pair-End library, following Illumina's genomic DNA library preparation procedure. Then the amplicon library was pair-end sequenced (2 × 250) on an Illumina MiSeq platform (Illumina, San Diego, CA, USA)), according to standard protocols. The raw data were deposited into the NCBI Sequence Read Archive database with accession number PRJNA754706.

2.4. Fluorescence Quantitative PCR (qPCR) Quantification of R. Solanacearum Density

QPCR was used to detect the abundance of fliC gene copies per gram of soil using a *R. solanacearum*-specific primer pair (forward primer: 5′-GAACGCCAACGGTGCGAACT-3′ and reverse primer: 5′-GGCGGCCTTCAGGGAGGTC-3′) [39]. The qPCR analyses were carried out using an Applied Biosystems 7500 Real-Time PCR System (Applied Biosystems, CA, USA) using the SYBR Green I fluorescent dye. Each reaction contained the following components: 10-μL SYBR Premix Ex Taq (TaKaRa Biotech. Co, Tokyo, Japan), 2-μL template, and 0.4-μL of both forward and reverse primers (10 mM each). The qPCR was performed by first denaturing for 30 s at 95 °C followed by cycling 40 times with a 5-s denaturizing step at 95 °C. Afterwards, a 34-s extension step was performed at 60 °C, followed by a melt curve analysis for 15 s at 95 °C, 1 min at 60 °C, and finally 15 s at 95 °C. Each sample had three technical replicates.

2.5. Bioinformatic Analysis

The raw data were treated with the Quantitative Insights into Microbial Ecology (QIIME) v1.9.1 (http://qiime.org/scripts/split_libraries_fastq.html, accessed on 20 October 2020), according to Caporaso et al. [40]. The USEARCH v6.1 (http://drive5.com/usearch/, accessed on 15 July 2020) was applied to identify and remove the chimeric reads [41]. Database sequences were aligned using MUSCLE (Version 3.8.31) (http://www.drive5.com/muscle/, accessed on 24 October 2020) [42]. Based on the 2,049,043 successfully aligned sequences, high-quality sequences were clustered into 4503 operational taxonomic units (OTUs) in de novo mode, based on 97% sequence similarity, using UCLUST (http://www.drive5.com/usearch, accessed on 1 October 2020) [41,43]. The taxonomic identity of each OTU was predicted based on similarity with the SILVA (Silva 132 release) (https://www.arb-silva.de/, accessed on 15 May 2020) database [43].

2.6. Predicted Bacterial Gene Function Changes Analysis

The Phylogenetic Investigation of Communities by Reconstruction of Unobserved States (PICRUSt) (http://picrust.github.com/picrust/, (accessed on 24 June 2019)) was further applied to predict metagenome functional content of 16S rRNA sequencing data [44].

Briefly, the OTU table was then delivered to PICRUSt v0.9.1 and the obtained functional predictions were made according to the metagenome inference workflow described by the developers [44].

2.7. The Analysis of Co-Occurrence Network

The random matrix theory (RMT)-based network approach was carried out to [45,46] explore co-occurrence network. The number of OTUs was filtered 1000 before uploading to the pipeline of local phylogenetic molecular ecological network analysis (MENA) (http://ieg4.rccc.ou.edu/mena, accessed on 21 July 2020). The OTUs from at least half of all the samples were retained, and some OTUs with missing values were kept blank. The similarity between the OTUs was calculated by the Pearson correlation coefficient method. The correlations of the correlation matrix were filtered more than 0.96 and p value was below 0.01. The network properties were calculated in local MENA. Then the constructed network was saved from pre-computed permutation and bootstrap files and then visualized in Cytoscape v3.5.1 (La, Jolla, San Diego, CA, USA) [47]. Different network nodes possessed distinct topological roles, which could be classified into two parameters, within-module connectivity (Zi) and among-module connectivity (Pi). In detail, the following groups were categorized: Peripherals (Zi $\leq$ 2.5, Pi $\leq$ 0.62), Connecters (Zi $\leq$ 2.5, Pi > 0.62), Module hubs (Zi > 2.5, Pi $\leq$ 0.62) and Network connectors (Zi > 2.5, Pi > 0.62).

2.8. The Calculation of Community Assembly Process

To quantify the assembly processes shaping the bacterial community within samples, the beta Nearest Taxon Index (βNTI) was calculated. The βNTI values measured the deviation of the β-mean nearest taxon distance (βMNTD) from the βMNTD of the null model, and were calculated using the 'comdist' function in Phylocom v4.2 in the 'picante' package in R v3.6.3. According to Stegen et al. [32], if $|\beta NTI|$ values were >2, deterministic processes played a key role in driving the microbial community. Conversely, if βNTI values were between -2 and +2, the microbial community structure was then dominated by stochastic processes. To further quantify the assembly processes, the RaupCrick metric (RCbray) was used to estimate pairwise microbial community turnover [32]. The pairwise comparisons, without deviating from the null model distribution, were considered the effects of dispersal limitation ($|\beta NTI| < 2$ and RCbray > +0.95) and homogenizing dispersal ($|\beta NTI| < 2$ and RCbray < -0.95) to community assembly, while RCbray values were below 0.95 indicating that community turnover between a given pair of communities was 'undominated' [32].

Normalized stochasticity ratio (NST) was further applied to identify the bacterial community assembly processes, where an index developed with 50% as the distinct point between more stochastic (>50%) assembly and more deterministic (<50%) [33]. This analysis was performed in the R v3.6.3 with the "NST" package [33].

2.9. Statistical Analysis

Alpha-diversity indices, including Richness, Shannon, and Chao 1 indices, and Faith's phylogenetic diversity (PD) were calculated using QIIME v1.9.1 to analyze bacterial diversity in all samples. Correlation analysis between each diversity index and *Rsol-fliC* gene copies, significance testing, and box plot illustration were all performed in IBM SPSS Statistics v21.0 (IBM Corp., Armonk, NY, USA). Based on the OTU table, the Principal Co-ordinates Analysis (PCoA) was carried out to compare the results of the Bray-Curtis distance-based using the 'ape' and 'vegan' package in R v3.6.3 (https://www.r-project.org/, accessed on 29 February 2020). The dominant classified family and COG categories using z-score transformed abundance data, and the results were plotted using the 'pheatmap' package in R v3.6.3.

3. Results

3.1. Plant Growth, Pathogen Density and Soil Properties

The average height of healthy tomato plants was 78.00 cm, while the average for the diseased ones was 68.63 cm, and there was no significance between them ($p > 0.05$, Table 1). Disease index of tomato bacterial wilt disease (BWD) in the diseased tomato plants was 83.33, which was significantly more severe than those of the healthy plants with disease index as low as 12.00 ($p < 0.01$; Table 1), demonstrating that there indeed existed severe bacterial wilt disease in the diseased tomato plants. The real-time PCR using *fliC* gene of *Ralstonia solanacearum* further highlighted the differences in the quantity of pathogens between diseased and healthy treatments ($p < 0.01$; Figure 1). According to the qPCR results, *R. solanacearum* could be detected in all samples (Figure 1). For different niches, the *fliC* gene copies per gram of soil ranging from $10^{3.09}$ (BSH) and $10^{4.56}$ (BSD) in bulk soil samples to $10^{5.57}$ (RSH) and $10^{7.42}$ (RSD) in rhizosphere samples, suggesting the population of *R. solanacearum* increased significantly from the bulk soil samples toward rhizosphere samples. Moreover, the pathogen density reached approximately 70.8-fold higher than that in RSD comparing to RSH (Figure 1).

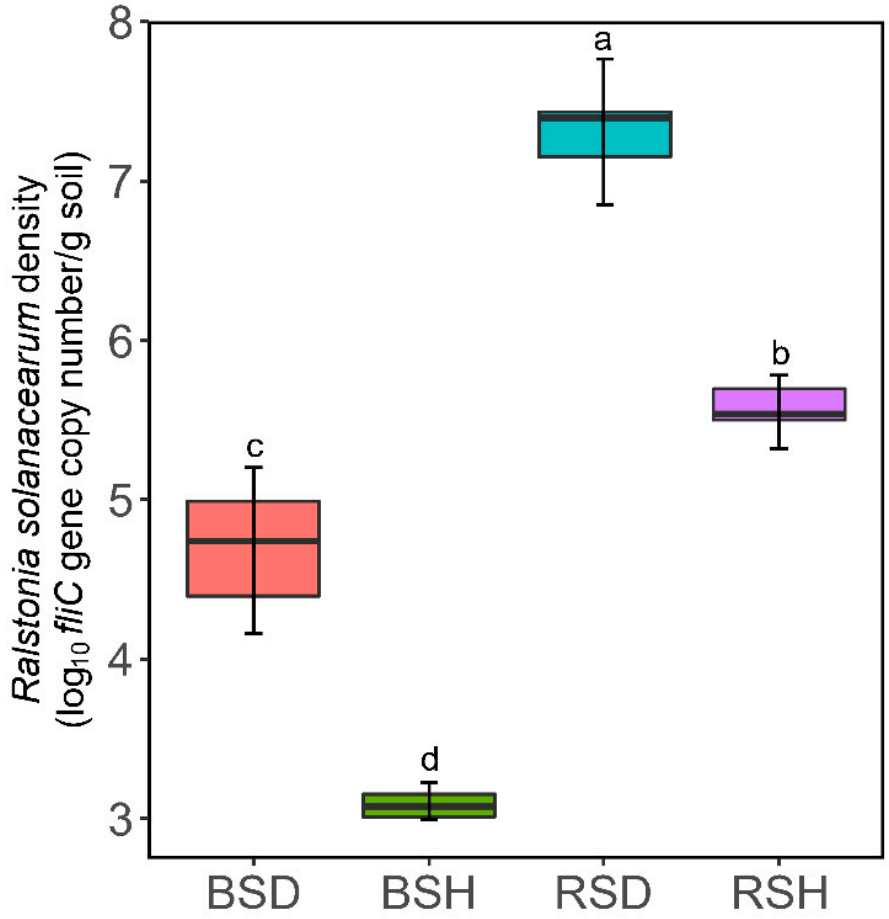

Figure 1. *Ralstonia solanacearum* density in the different samples. Different letters indicated a significant difference ($p < 0.05$). BSH: healthy bulk soil samples; BSD: diseased bulk soil samples; RSH: healthy rhizosphere soil samples; RSD: diseased rhizosphere soil samples.

Of all the measured soil physicochemical properties, soil moisture content, Ec, and NO_3^--N, as well as exchangeable NH_4^+-H, in the RSH samples were significantly lower than those in the diseased samples ($p < 0.05$; Table 1). In contrast, the soil organic carbon (SOC), pH, and available potassium (AK) were significantly higher in the healthy samples in relation to the diseased samples ($p < 0.05$). For example, the SOC content in healthy samples was 8.97 g kg^{-1} which was obviously higher than that in diseased samples (Table 1).

Furthermore, soil moisture, pH, NO_3^--N, NH_4^+-N, SOC, AK, and Ec obviously correlated with pathogen densities ($p < 0.05$; Figure S1). Other soil physicochemical factors, such as the content of total nitrogen (TN), total phosphorus (TP), and total potassium (TK), as well as available phosphorus (AP) content, did not significantly vary across healthy samples and diseased samples ($p > 0.05$).

Table 1. Tomato plant and soil chemical properties.

Properties	Diseased Samples	Healthy Samples
Plant		
Plant height (cm)	68.63 ± 4.93 a	78.00 ± 6.57 a
Disease index (%)	83.33 ± 0.06 a	12.50 ± 0.05 b
Soil		
moisture	0.14 ± 0.01 a	0.08 ± 0.01 b
pH	6.20 ± 0.09 b	6.61 ± 0.03 a
Ec (mS cm^{-1})	0.30 ± 0.03 a	0.19 ± 0.01 b
NO_3^--N (mg kg^{-1})	45.68 ± 4.11 a	19.13 ± 3.41 b
NH_4^+-N (mg kg^{-1})	14.23 ± 0.28 a	10.92 ± 0.77 b
SOC (g kg^{-1})	7.67 ± 0.18 b	8.97 ± 0.14 a
TN (g kg^{-1})	1.38 ± 0.04 a	1.33 ± 0.06 a
TP (g kg^{-1})	1.34 ± 0.03 a	1.30 ± 0.07 a
TK (g kg^{-1})	15.54 ± 0.34 a	15.08 ± 0.25 a
AP (mg kg^{-1})	116.47 ± 5.91 a	97.78 ± 7.83 a
AK (mg kg^{-1})	270.33 ± 5.11 b	316.20 ± 18.51 a

Values are means ± standard error. Different lowercase letters indicated a significant difference ($p < 0.05$) between diseased samples and healthy samples. EC for electrical conductivity, SOC for soil organic carbon; TN for total nitrogen, TP for total phosphorus, TK for total potassium, NO_3^--N for nitrate, NH_4^+-N for ammonium, AP for available phosphorus and AK for available potassium.

3.2. Microbial Composition, Diversity and Community Structure in Response to BWD

There were 655,488 sequences obtained from 24 samples, out of which 4503 OTUs were classified into 833 genera belonging to 30 phyla. The top 10 dominant phyla, class, family, and genera in all samples were displayed (Figure S2). The relative abundance of the dominant phyla, class, family, and genera differed in the rhizosphere soil samples (RSD and RSH), while no discrepancy was observed in the bulk soil samples (BSD and BSH) (Figure S2), which indicated that the difference in microorganisms was mainly reflected in the rhizosphere, rather than the bulk soil, during the occurrence of bacterial wilt. Significantly more abundance of the family Chitinophagaceae, Streptomycetaceae, and genera *Burkholderia*, *Streptomyces*, and *Bacillus* were observed in the RSH, while there was more abundance of *Ralstonia* in the RSD (Figures 2 and S2).

The bacterial alpha diversities, including Richness, Shannon, Chao 1 indices, and Faith's PD, were significantly different between the rhizosphere and bulk soil samples ($p < 0.05$), and the rhizosphere samples had lower alpha diversity than that in the bulk soil samples. These results indicated that the farther the distance from the plant root, the higher bacterial diversity was. Like bacterial community composition, the diversity in bulk soil samples also exhibited no significant differences between the BSD and BSH (Table 2). However, apparent difference was observed in the rhizosphere samples with higher alpha diversity observed in the RSH (Table 2). Except for the alpha diversity, an obvious difference in bacterial community structure existed in all samples evaluated through principal coordinates analysis (PCoA) and community similarity analysis (PERMANOVA) ($p < 0.001$) (Figure 3A,D). According to the PCoA analysis, bacterial communities distinctly clustered by soil niches (rhizosphere and bulk soil) ($p < 0.05$; Figure 3A). The horizontal and vertical axis of the PCoA explained 63.9% and 12.3% of the total variability in the bacterial communities, respectively. Furthermore, within similar niches, bacterial communities in rhizosphere samples could be distinguished, based on pathological status (RSD and

RSH) ($p < 0.05$; Figure 3C), while this was not the case with regards to bulk soil samples ($R = -0.046$, $p > 0.05$; Figure 3B).

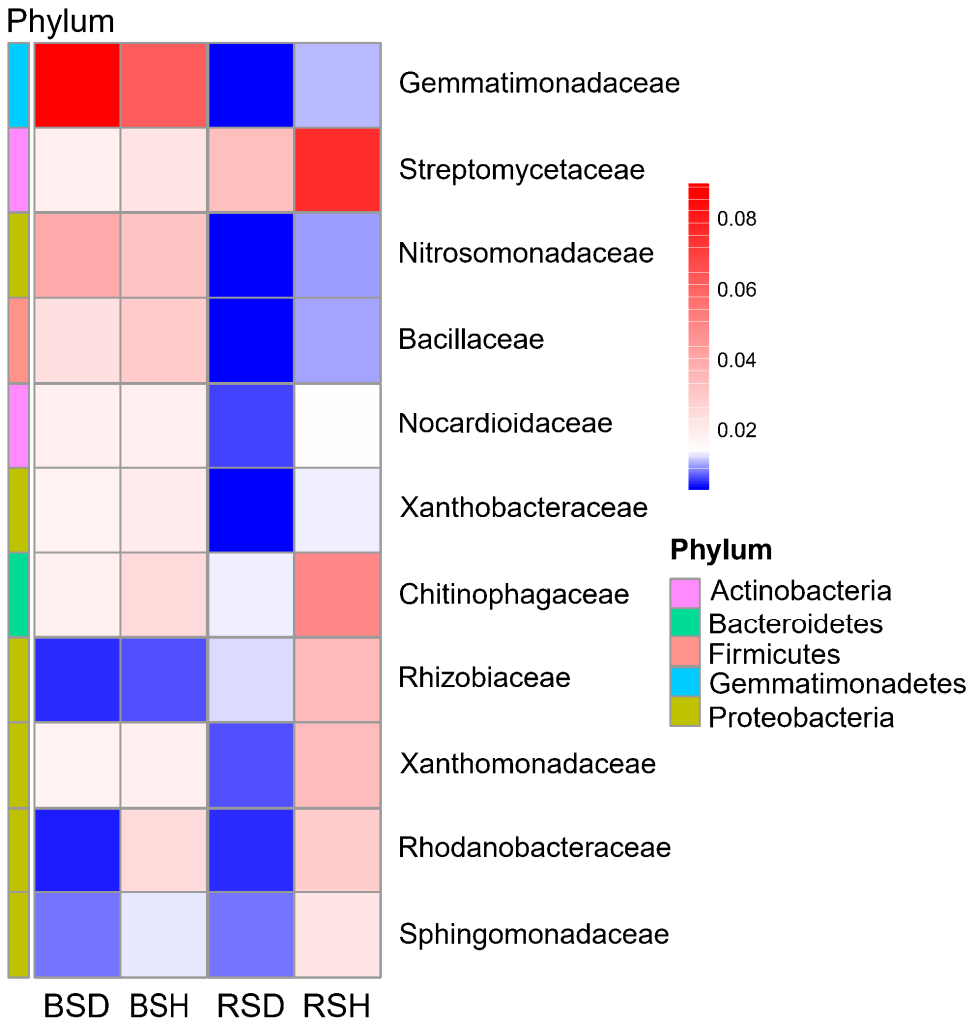

Figure 2. Heatmap of bacterial families in different treatments clustered based on complete-linkage hierarchical clustering of Euclidean distances. BSH: healthy bulk soil samples; BSD: diseased bulk soil samples; RSH: healthy rhizosphere soil samples; RSD: diseased rhizosphere soil samples.

Table 2. The diversity of microbial community in different samples.

Sample	Richness	Shannon	Chao 1	Faith's PD
BSD	2151 ± 75 a	9.15 ± 0.07 a	2796 ± 88 a	114 ± 4.37 a
BSH	2119 ± 108 a	9.10 ± 0.16 a	2702 ± 135 a	150 ± 6.14 a
RSD	912 ± 71 c	2.79 ± 0.29 c	1481 ± 101 c	78 ± 4.45 c
RSH	1515 ± 70 b	7.02 ± 0.26 b	2117 ± 144 b	116 ± 4.67 b

Values are means ± standard error. Different letters within the same column indicated a significant difference ($p < 0.05$; lowercase). BSH: healthy bulk soil; BSD: diseased bulk soils samples; RSH: healthy rhizosphere soil samples; RSD: diseased rhizosphere soils samples.

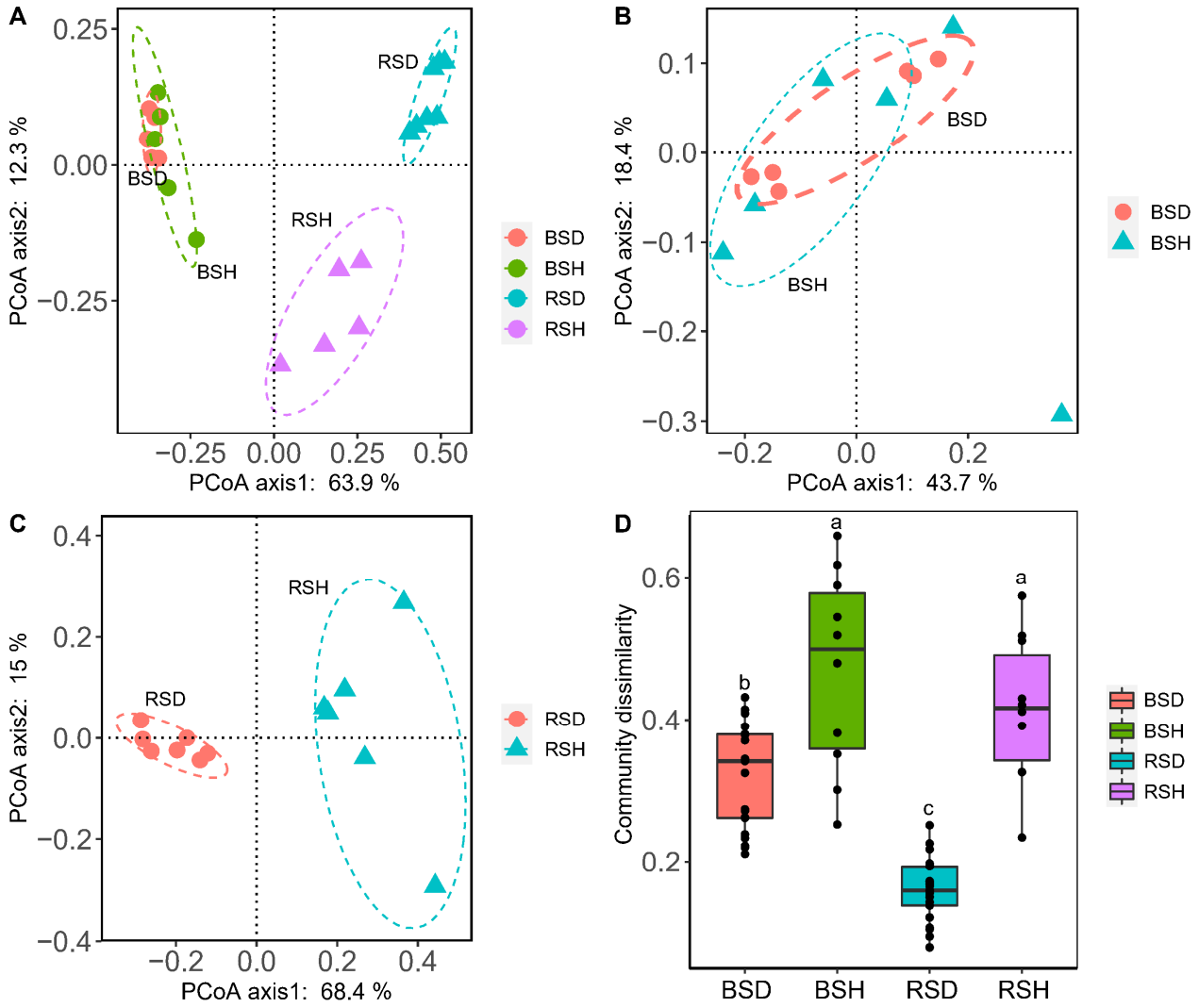

Figure 3. Principal Coordinates Analysis (PCoA) and community distance analysis based at OTU level. (**A**) PCoA of bacterial community composition in all treatments. (**B**) PCoA of bacterial community composition in bulk soil samples. (**C**) PCoA of bacterial community composition in rhizosphere soil samples. Panel (**D**) Community dissimilarity among all samples. Different lowercase letters indicated a significant difference ($p < 0.05$). BSH: healthy bulk soil samples; BSD: diseased bulk soil samples; RSH: healthy rhizosphere soil samples; RSD: diseased rhizosphere soil samples.

3.3. Influences of BWD on the Microbial Function

The PCoA analysis, based on the COG function profiles, indicated that the function varied in different rhizosphere bacterial communities (PERMANOVA, $p < 0.001$) (Figure S3). There were some significantly enriched and depleted COG profiles between the RSD and RSH samples (Figure 4). The RSD mainly contained functional gene profiles, such as those connected with translation, energy production and conversion, amino acid transport, secondary metabolites biosynthesis, lipid transport, and bacterial metabolism. However, some functional gene classes, including carbohydrate transport, cytoskeleton, defense mechanisms, and extracellular structures, were enriched in the RSH samples (Figure 4).

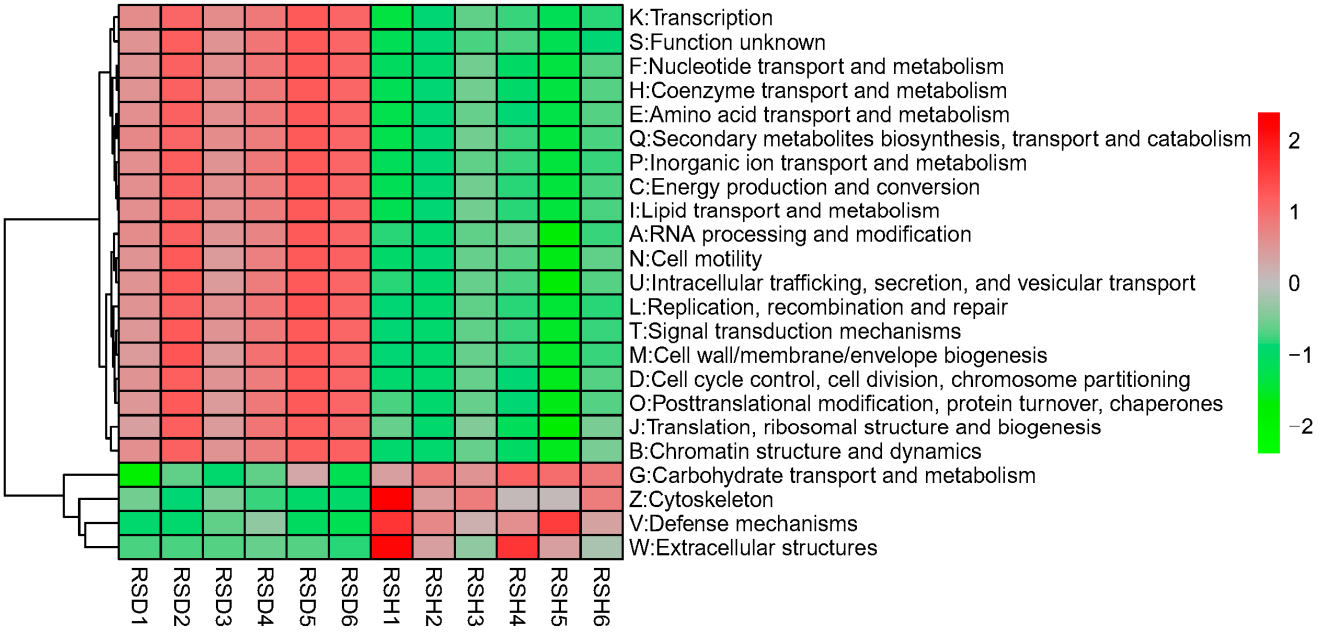

Figure 4. The COG function profiles in all rhizosphere samples. RSD stood for diseased rhizosphere soil samples, and RSH for healthy rhizosphere soil samples.

3.4. Influences of BWD on the Microbial Co-Occurrence Network

The co-occurrence networks were constructed based on OTU level to explore the difference in bacterial co-occurrence patterns among four treatments. Topological indexes showed that all networks fitted well as R^2 of power-law ranged from 0.811 to 0.901. Among them, the network indicators, including the total links, average degree (avgK), total nodes, density, and connectedness (Con) index, successfully characterized the complexity of each network (Figure 5; Table S1). The networks differed between diseased and healthy samples. The BSH and RSH networks possessed higher complexities, while the RSD had the least complexity. Low values of transitivity (Trans) were observed in the BSD and RSD networks, while other network indicators, such as high values of Con, more nodes, links, average clustering coefficient (avgCC), and density, were observed in the healthy samples (BSH and RSH). Furthermore, according to the Zi (a value measuring within-module connectivity) and Pi (a value measuring among-module connectivity) calculated by the network analysis, there were 4.44%, 2.49% nodes fell into network connectors ($Zi > 2.5$, $Pi > 0.62$) in the BSH and RSH networks, respectively, which were higher than that in the BSD and RSD samples (1.19% in BSD and 0.75% in RSD) (Figure S4). The above results suggested that the healthy samples tended to form a stable and complicated bacterial community network.

3.5. Bacterial Community Assembly Processes in Response to the BWD

Based on the neutral-based models' analysis, the R^2 for BSD, BSH, RSD, and RSH were 0.66, 0.607, 0.63, and 0.601, respectively, which reflected good model prediction (Figure S5). The m value (migration rate) tended to decrease from diseased samples to healthy samples, suggesting that diseased samples were more highly diffused than healthy samples.

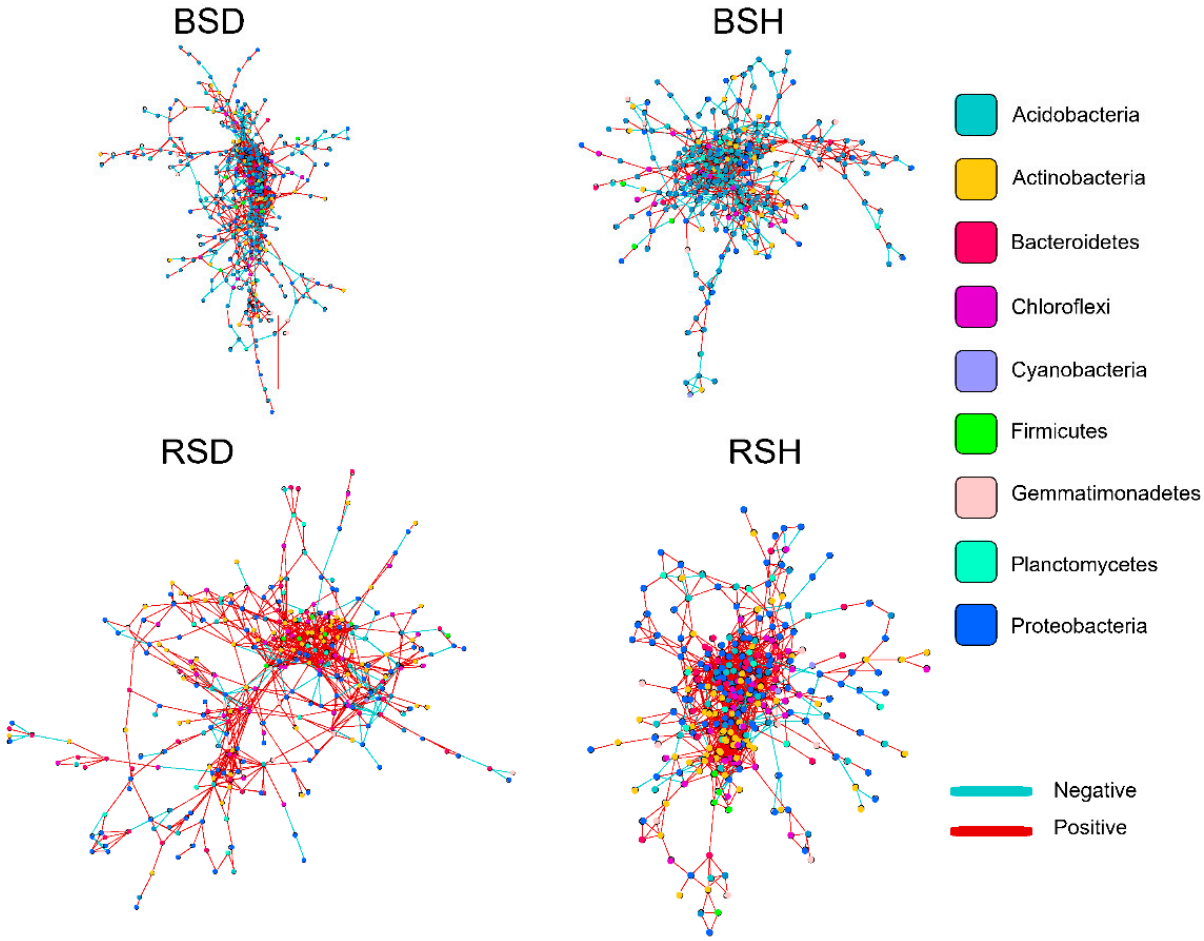

Figure 5. The Co-occurrence network of bacterial community at OTU level in all treatments. BSH: healthy bulk soil samples; BSD: diseased bulk soil samples; RSH: healthy rhizosphere soil samples; RSD: diseased rhizosphere soil samples.

To quantify the relative contributions of stochastic and deterministic assembly processes shaping bacterial community among different treatments, the beta Nearest Taxon Index (βNTI) and normalized stochasticity ratio (NST) were calculated within each treatment (Figure 6A). The community assembly processes in the diseased samples were dominated by the deterministic process (the value of $|\beta NTI| > 2$), in which the determinism in RSD and BSD samples reached 66.67% and 40%, respectively. On the other hand, community assembly processes in the healthy samples were dominated by the stochastic process (the value of $|\beta NTI| > 2$), and the stochasticity (the value of $|\beta NTI| < 2$) (66.67% and 90% respectively) in the BSH and RSH samples became the dominant factor to drive the community. In detail, it is found that homogeneous selection dominated the deterministic process in RSD (Figure 6B), while RSH and BSH had higher strengths of dispersal limitation. Furthermore, it was observed that βNTI was also significantly decreased with increase of *R. solanacearum*'s density (Figure S6A). Mantel tests also demonstrated that the change of genus *Ralstonia* abundance significantly affected the assembly processes of the bacterial community (Mantel $R = -0.659$, Figure S6B). The relative contributions of homogeneous selection in the deterministic process also increased with change in pathogen density in the rhizosphere samples, while the opposite occurred with the contribution of dispersal limitation.

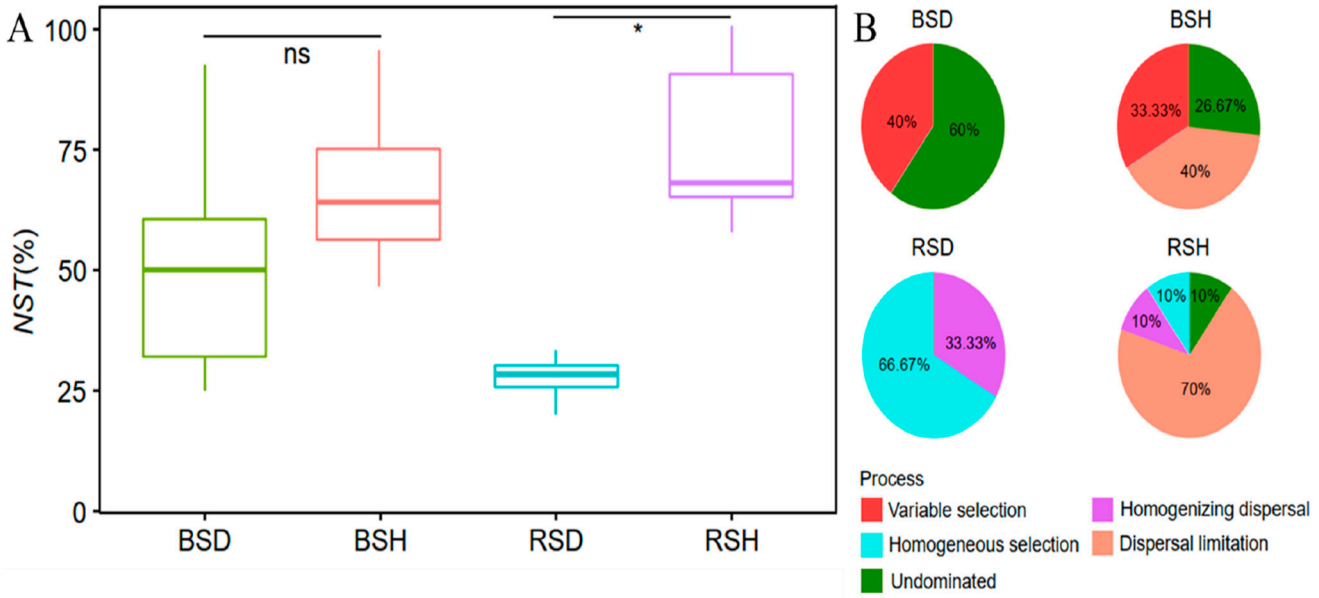

Figure 6. The bacterial community assembly processes across all the treatments. (**A**) The normalized stochasticity ratio (NST) was developed based on bray-curtis distance (NSTbray) with 50% as the boundary point between more deterministic (50%) and more stochastic (50%) assembly. (**B**) The community assembly processes in all treatments. "ns" indicated there was no difference between the BSD and BSH. "*" indicated a significant difference ($p < 0.05$) between the RSD and RSH samples. BSH: healthy bulk soil samples; BSD: diseased bulk soil samples; RSH: healthy rhizosphere soil samples; RSD: diseased rhizosphere soil samples.

4. Discussion

In this study, soil physicochemical properties were identified in relation to the invasion of soil-borne pathogens into host plants. The physicochemical properties of soil altered between healthy and diseased samples and were closely correlated with pathogen densities (Table 1). The pH, moisture content, ammonium, and nitrate content decreased compared to the healthy samples, while SOC and AK contents increased. High temperature and humidity conditions provide convenience for BWD occurrence and rapid spread [13,18]. More available carbon resources in the soil were significantly negatively correlated with growth of the pathogen, while more ammonium could help in pathogen growth [48–50]. During the invasion of the pathogen on the host plant roots and xylem, nitrate availability was thought to be important for the expression of the *R. solanacearum* virulence gene, and thus it could influence pathogen pathogenicity without impacting on pathogen density [48,51]. Similarly, higher humidity, ammonium, and nitrate content, lower pH and concentration of carbon were found in the RSD samples in this study (Table S1). In addition to abiotic factors, biotic factors prompt bacterial wilt outbreaks [13]. According to the Mantel test between bacterial community structures and soil/microbial properties, pathogen abundance had more effect on bacterial community structure, indicating that bacterial communities may be more strongly affected by biotic factors than abiotic factors (Table S2). Therefore, these results indicate that such shifts in bacterial community structure were caused by invasion of the *R. solanacearum*, which either drove the recruitment of beneficial bacteria or promoted resistance to bacterial wilt.

4.1. The Effect of Increased Pathogen Density on the Bacterial Community Composition

Revealing the potential sources of microbiomes could provide some crucial information on interactions among plants, soil, and microbes [7,52]. The bacterial community composition in the bulk soil (BSD and BSH) was similar on different taxa. However, there were significant differences in the composition of the rhizosphere microbial community (Figure S2). No difference being observed in community composition may be due to less sensitivity

to pathogen invasion in the bulk soil microbiome compared to the rhizosphere. Various studies found that host plant roots could be stimulated to recruit some beneficial microbes to the rhizosphere through releasing root exudates when infected by soil-borne pathogens, and these compositional changes thus inhibiting the growth of pathogens [17,53,54]. It was similar for the family taxa, including Chitinophagaceae, Bacillaceae, Streptomycetaceae, and Xanthomonadaceae, and the genus, including *Streptomyces, Bacillus, Burkholderia*, and *Subgroup_6*, found to be enriched in RSH, while the pathogen genus *Ralstonia* was significantly increased in RSD instead (Figure S2). The Streptomycetaceae family and *Streptomyces* genus, belonging to the Actinobacteria phylum, known to produce clinical antibiotics [55], may directly suppress the growth of the pathogen *R. solanacearum* [56]. The abundance of the family Bacillaceae and the genus *Bacillus*, belonging to the phylum Firmicutes, were also known for their antagonism by producing the lipopeptide antibiotics to defend against pathogen *R. solanacearum* growth [57]. As for the genus *Burkholderia,* it could act as an antagonist of soil-borne pathogens [10]. Moreover, the Xanthomonadales could produce volatile organic compounds which could help to inhibit the invasion of plant soil-borne pathogens, and were found to have an abundant enrichment in healthy rhizosphere samples [58]. However, some beneficial microbes, genus *Bacillus* and *Burkholderia*, were also found in the diseased rhizosphere. Thus, the enrichment of these beneficial microbes, such as *Bacillus* and *Streptomyces*, in the rhizosphere may be why tomato plants in RSH remained healthy [17].

Bacterial community diversity could influence antagonistic or facilitative interactions between host plants and pathogens [59,60]. The lower population of *R. solanacearum* in the RSH could attribute to the prevalence of beneficial microbes. Numerous studies suggest that higher microbial diversity could help host plants defend against soil-borne pathogen invasion and thus increase their resistance to pathogens [14,61]. In this study, the bacterial diversity of RSH was higher than that of RSD. However, bacterial diversity decreased gradually from bulk soils toward rhizosphere soils, indicating the existence of strong root filtration [13]. Over and above bacterial community diversity, pathogen invasion also significantly influences bacterial community structures. According to the PCoA results, rhizosphere soil samples and bulk soil samples could be distinguished according to different niches, and there were significant differences between the RSH and RSD in rhizosphere soils, while no significant differences were detected in bulk soils (Figure 2, Table S2). Moreover, an obvious distance-decay relationship existed between the variation of pathogen abundance and the community dissimilarity (Figure S7). With the increase of pathogen abundance, the variation of bacterial community structure (paired Bray-Curtis distance) also increased significantly.

Apart from compositional changes, we also observed that the complexity of the bacterial community co-occurrence network reduced and there was loss of various sub-network connectors according to the properties of the networks in the diseased samples. A complex community network was usually more resistant to external stress [15,62], thus complex networks in RSH could better defend against soil-borne pathogen invasion. Moreover, bacterial functions based on the COG profiles also changed, demonstrating that some functional gene classes associated with plant soil-borne pathogen defense, including carbohydrate transport (G gene) and defense mechanisms, were enriched in the RSH (Figure 4), which was consistent with Xiong's results [63]. It was found that higher carbohydrate transport activity in healthy rhizosphere soil might contribute to abundant resources being available for microbes in these soils. Secondary metabolites biosynthesis (Q gene) was related with the pathogen *R. solanacearum*. Less defense mechanism related genes in the diseased rhizosphere soils indicated its weak resistance to pathogen infection [63–65]. Together, the above results indicated that the bacterial community diversity was related to the loss of bacterial composition, which potentially led to expressions of microbial functions related to soil-borne pathogen suppression.

4.2. Increased Pathogen Density Altered the Relative Contribution of Stochastic and Deterministic Processes

It is quite important to reveal the mechanisms of microbial community assembly in microbial ecology [66]. The microbial community was affected by different microbial ecological mechanisms; therefore, it was important to identify the relative impact of deterministic and stochastic processes on community assembly [67]. Microbial communities associated with stochastic processes often exhibited greater diversity than communities associated with deterministic processes, thus had better resistance to environmental stress [25] The above perspective was consistent with the findings of our study, reporting that the RSH samples had more community diversity and the bacterial community assembly was dominated by the stochastic processes, according to the two community assembly methods (βNTI and NST). In addition, more deterministic processes were observed in the RSD samples, while relatively less deterministic processes were observed in the RSH samples, which indicated that pathogen invasion, as a major biotic factor, could be a driver of bacterial community assembly processes.

4.3. The Effect of Homogeneous Selection on Bacterial Community

To better understand microbial ecology in more detail, it was vital to reveal the potential factors influencing the relative contributions of stochastic and deterministic assembly processes driving microbial communities [20,30]. Recent studies demonstrated that soil pH, available sulfur, and salinity are the vital factors affecting microbial community assembly processes [30,31,68]. However, there were few studies on biotic factors, such as soil-borne pathogen infection, affecting the relative contributions of stochastic and deterministic processes controlling the assembly of bacterial communities under soil borne pathogen invasion. We found that the community assembly processes transformed towards determinism (homogeneous selection) along with increasing pathogen abundance, which further increased structural difference among the bacterial community (Figures 6, S6 and S7). Moreover, the increased homogeneous selection in community assembly processes enhanced the distance-decay relation and led to more discrepancy in the bacterial community structures because of the selective environments (biotic factors). The increase in *R. solanacearum* density decreased the extent of phylogenetic clustering in the microbial community and *R. solanacearum* density might play vital roles in affecting the balance between stochastic and deterministic assembly for bacterial communities. Homogenizing selection dominated the community assembly in RSD, indicating that there existed strong environmental selection and this environmental selection might be the role of soil borne pathogens. Thus, we guessed that there were two mechanisms explaining how pathogens affected bacterial community assembly: (a) directly affecting the growth of other non-pathogenic bacteria, and (b) interacting with host plants to indirectly affect the bacterial community assembly. Though the soil-borne pathogen invasion was known to affect bacterial community composition, diversity, and function [36,65], it had not been clear how pathogens mediated bacterial community assembly processes. Here, our results demonstrated that there were more deterministic assembly processes shaping the diseased bacterial community, while stochastic assembly processes dominated the healthy bacterial community. Potential mechanisms were likely related to the changes in community assembly processes responding to the variation of soil-borne pathogen density. Firstly, more abundance of pathogens colonized in diseased soils and then imposed more resource limitation on beneficial microbes, which might exclude and reduce the colonization of these beneficial bacteria to a greater extent and therefore led to an increased effect of deterministic processes [20]. Secondly, healthy rhizospheres harbored more microbes and had a more stable and complicated co-occurrence network, which could strengthen the dispersion of microorganisms, thereby, in turn, increasing the advantages of stochastic processes [27]. Additionally, the increased stochasticity suggested that healthy rhizospheres could then better adapt to environmental stress, such as soil borne pathogen invasion. Our findings revealed important links between

soil borne pathogen infection and bacterial community assembly, which might help deepen understanding of how these link to microbial diversity and soil ecosystem processes.

5. Conclusions

Tomato plants shape healthy rhizosphere bacterial communities by attracting some potential bacterial antagonists when infected by soil-borne pathogens. Higher bacterial community diversity and a more complicated bacterial community co-occurrence network were displayed in the healthy samples to further defend against soil-borne pathogen invasion. Moreover, variation in bacterial community compositions led to upregulation of functional gene profiles associated with plant pathogen defense in healthy rhizosphere soil. In addition, deterministic processes drove the bacterial community under pathogen invasion. The bacterial community assembly was driven by the soil-borne pathogen invasion promoting the bacterial community assembly's transformation from stochastic process to deterministic process. Through various analytical methods, our results provided some important insights into the response of bacterial community composition, diversity, structure, function, co-network and assembly processes to soil-borne pathogen invasion, which would deepen our comprehension on how agricultural ecosystems may respond to soil borne pathogen invasion under long term continuous cropping.

Supplementary Materials: The following supporting information can be downloaded at: https://www.mdpi.com/article/10.3390/agronomy12051024/s1, Figure S1 Correlations between soil chemical properties and microbial properties. Ec for electrical conductivity, SOC for soil organic carbon; TN for total nitrogen, TP for total phosphorus, TK for total potassium, NO_3^--N for nitrate, NH_4^+-N for ammonium, AP for available phosphorus, AK for available potassium, DSI for disease index. Different lowercase letters indicated significant distinctions among different treatments ($p < 0.05$), Figure S2 The relative abundance of dominant bacterial groups at the phylum (**A**), class (**B**), family (**C**), and genus (**D**) level in different treatments. Note: "*" indicated significant differences and "ns" indicated there was no significance at the 0.05 level. BSH: healthy bulk soil samples; BSD: diseased bulk soil samples; RSH: healthy rhizosphere soil samples; RSD: diseased rhizosphere soil samples, Figure S3 Principal Coordinates Analysis (PCoA) based on COG function genes between RSD and RSH. RSD stood diseased rhizosphere soil samples, and RSH for healthy rhizosphere soil samples, Figure S4 The co-occurrence network roles of analyzing module feature at OTU level in all treatments. BSD for A, BSH for B, RSD for C, and RSH for D. BSH: healthy bulk soil samples; BSD: diseased bulk soil samples; RSH: healthy rhizosphere soil samples; RSD: diseased rhizosphere soil samples, Figure S5 Fit of the neutral community model (NCM) of community assembly in the BSD (**A**), BSH (**B**), BS (**C**), RSD (**D**), RSH (**E**), and RS (**F**). The predicted occurrence frequencies for all treatments. The solid blue lines indicated the best fit to the NCM, and the dashed blue lines represent 95% confidence intervals around the model prediction. OTUs that occurred more or less frequently than predicted by the NCM are shown in different colors. m indicates the immigration rate, R^2 indicated the fit to this model. BSH: healthy bulk soil samples; BSD: diseased bulk soil samples; RSH: healthy rhizosphere soil samples; RSD: diseased rhizosphere soil samples. RS: rhizosphere soil; BS: bulk soil, Figure S6 The distance-decay relationship between changes in pathogen density and βNTI. Data were fitted using linear regression and examined by Mantel test, Figure S7 The distance-decay relationship between changes in pathogen density and community distance. Data were fitted using linear regression and examined by Mantel test. Table S1 The bacterial co-occurrence network properties in all treatments, Table S2 The mantel test between community distance and soil properties.

Author Contributions: Y.D., J.L. and H.L. designed the experiment; H.L., F.S., J.P. and M.S. performed the experiments; H.L. analyzed the data; H.L. and J.L. interpreted the data and wrote the paper. All authors have read and agreed to the published version of the manuscript.

Funding: This study was supported by the National Natural Science Foundation of China (No. 41977055), National Key Research and Development Program of China (2017YFD0200604, 2016YFD0200305).

Institutional Review Board Statement: This article does not contain any studies with human participants or animals performed by any of the author.

Data Availability Statement: The raw data were deposited into the NCBI (https://www.ncbi.nlm.nih.gov/, accessed on 15 August 2021) Sequence Read Archive database with accession number PRJNA754706.

Acknowledgments: The authors would like to thank students coming from CAS Key Laboratory of Soil Environment and Pollution Remediation for their assistance in the data analyzing and paper writing.

Conflicts of Interest: The authors declare no conflict of interest.

References

1. Bailey, K.; Lazarovits, G. Suppressing soil-borne diseases with residue management and organic amendments. *Soil Till. Res.* **2003**, *72*, 169–180. [CrossRef]
2. Wu, H.; Gao, Z.; Zhou, X.; Shi, X.; Wang, M.; Shang, X.; Liu, Y.; Gu, D.; Wang, W. Microbial dynamics and natural remediation patterns of Fusarium-infested watermelon soil under 3-yr of continuous fallow condition. *Soil Use Manag.* **2013**, *29*, 220–229. [CrossRef]
3. Hayward, A.C. Biology and Epidemiology of Bacterial Wilt Caused by *Pseudomonas solanacearum*. *Annu. Rev. Phytopathol.* **1991**, *29*, 65–87. [CrossRef]
4. Raaijmakers, J.M.; Paulitz, T.C.; Steinberg, C.; Alabouvette, C.; Moenne-Loccoz, Y. The rhizosphere: A playground and battlefield for soilborne pathogens and beneficial microorganisms. *Plant Soil* **2009**, *321*, 341–361. [CrossRef]
5. Garbeva, P.; Veen Jorge, J.A.; van Elsas, J. Microbial diversity in soil: Selection of the microbial populations by plant and soil type and implementations for disease suppressiveness. *Annu. Rev. Phytopathol.* **2004**, *42*, 243–270. [CrossRef] [PubMed]
6. Mendes, L.; Raaijmakers, J.; Hollander, M.; Mendes, R.; Tsai, S. Influence of resistance breeding in common bean on rhizosphere microbiome composition and function. *ISME J.* **2017**, *12*, 212–224. [CrossRef] [PubMed]
7. Bulgarelli, D.; Schlaeppi, K.; Spaepen, S.; van Themaat, E.V.L.; Schulze-Lefert, P. Structure and Functions of the Bacterial Microbiota of Plants. *Annu. Rev. Plant Biol.* **2013**, *64*, 807–838. [CrossRef]
8. Castrillo, G.; Teixeira, P.J.; Herrera Paredes, S.; Law, F.; Lorenzo, L.; Feltcher, M.; Finkel, O.; Breakfield, N.; Mieczkowski, P.; Jones, C.; et al. Root microbiota drive direct integration of phosphorus stress and immunity. *Nature* **2017**, *543*, 513–518. [CrossRef]
9. Mendes, R.; Garbeva, P.; Raaijmakers, J.M. The rhizosphere microbiome: Significance of plant beneficial, plant pathogenic, and human pathogenic microorganisms. *FEMS Microbiol. Rev.* **2013**, *37*, 634–663. [CrossRef]
10. Carrión, V.; Perez-Jaramillo, J.E.; Cordovez, V.; Tracanna, V.; de Hollander, M.; Ruiz-Buck, D.; Mendes, L.W.; van Ijcken, W.F.J.; Gomez-Exposito, R.; Elsayed, S.S.; et al. Pathogen-induced activation of disease-suppressive functions in the endophytic root microbiome. *Science* **2019**, *366*, 606–612. [CrossRef]
11. Mendes, R.; Kruijt, M.; de Bruijn, I.; Dekkers, E.; van der Voort, M.; Schneider, J.H.; Piceno, Y.M.; DeSantis, T.Z.; Andersen, G.L.; Bakker, P.A.; et al. Deciphering the rhizosphere microbiome for disease-suppressive bacteria. *Science* **2011**, *332*, 1097–1100. [CrossRef] [PubMed]
12. Philippot, L.; Raaijmakers, J.M.; Lemanceau, P.; Van, D.P.; Wim, H. Going back to the roots: The microbial ecology of the rhizosphere. *Nat. Rev. Microbiol.* **2013**, *11*, 789–799. [CrossRef] [PubMed]
13. Van Elsas, J.D.; Kastelein, P.; De Vries, P.M.; van Overbeek, L. Effects of ecological factors on the survival and physiology of *Ralstonia solanacearum* bv. 2 in irrigation water. *Can. J. Microbiol.* **2001**, *47*, 842–854. [CrossRef]
14. Van Elsas, J.D.; Chiurazzi, M.; Mallon, C.A.; Elhottovā, D.; Kristůfek, V.; Salles, J.F. Microbial diversity determines the invasion of soil by a bacterial pathogen. *Proc. Natl. Acad. Sci. USA* **2012**, *109*, 1159–1164. [CrossRef] [PubMed]
15. Wei, Z.; Yang, T.; Friman, V.P.; Xu, Y.; Shen, Q.; Jousset, A. Trophic network architecture of root-associated bacterial communities determines pathogen invasion and plant health. *Nat. Commun.* **2015**, *6*, 8413. [CrossRef]
16. Tilman, D. Niche tradeoffs, neutrality, and community structure: A stochastic theory of resource competition, invasion, and community assembly. *Proc. Natl. Acad. Sci. USA* **2004**, *101*, 10854–10861. [CrossRef]
17. Berendsen, R.; Pieterse, C.; Bakker, P. The rhizosphere microbiome and plant health. *Trends Plant Sci.* **2012**, *17*, 478–486. [CrossRef]
18. Wei, Z.; Huang, J.; Yang, T.; Jousset, A.; Xu, Y.; Shen, Q.; Friman, V.P. Seasonal variation in the biocontrol efficiency of bacterial wilt is driven by temperature-mediated changes in bacterial competitive interactions. *J. Appl. Ecol.* **2017**, *54*, 1440–1448. [CrossRef]
19. Mallon, C.; Poly, F.; Roux, X.; Marring, I.; Elsas, J.A.N.; Salles, J. Resource pulses can alleviate the biodiversity–invasion relationship in soil microbial communities. *Ecology* **2015**, *96*, 915–926. [CrossRef]
20. Feng, Y.; Chen, R.; Stegen, J.; Guo, Z.; Zhang, J.; Li, Z.; Lin, X. Two key features influencing community assembly processes at regional scale: Initial state and degree of change in environmental conditions. *Mol. Ecol.* **2018**, *27*, 5238–5251. [CrossRef]
21. Liu, W.B.; Graham, E.; Zhong, L.; Zhang, J.; Li, W.; Li, Z.; Lin, X.; Feng, Y. Dynamic microbial assembly processes correspond to soil fertility in sustainable paddy agroecosystems. *Funct. Ecol.* **2020**, *34*, 1244–1256. [CrossRef]
22. Mendes, L.W.; Kuramae, E.E.; Navarrete, A.A.; van Veen, J.A.; Tsai, S.M. Taxonomical and functional microbial community selection in soybean rhizosphere. *ISME J.* **2014**, *8*, 1577–1587. [CrossRef] [PubMed]
23. Dumbrell, A.; Nelson, M.; Helgason, T.; Dytham, C.; Fitter, A. Relative roles of niche and neutral processes in structuring a soil microbial community. *ISME J.* **2010**, *4*, 337–345. [CrossRef] [PubMed]

24. Langenheder, S.; Székely, A. Species sorting and neutral processes are both important during the initial assembly of bacterial communities. *ISME J.* **2011**, *5*, 1086–1094. [CrossRef]
25. Graham, E.B.; Crump, A.R.; Resch, C.T.; Fansler, S.J.; Arntzen, E.V.; Kennedy, D.W.; Fredrickson, J.K.; Stegen, J.C. Deterministic influences exceed dispersal effects on hydrologically-connected microbiomes. *Environ. Microbiol.* **2017**, *19*, 1552–1567. [CrossRef]
26. Zhou, J.; Liu, W.; Ye, D.; Jiang, Y.H.; Wang, A. Stochastic Assembly Leads to Alternative Communities with Distinct Functions in a Bioreactor Microbial Community. *MBio* **2013**, *4*, e00584-12. [CrossRef] [PubMed]
27. Dini-Andreote, F.; Stegen, J.; Elsas, J.; Salles, J. Disentangling mechanisms that mediate the balance between stochastic and deterministic processes in microbial succession. *Proc. Natl. Acad. Sci. USA* **2015**, *112*, E1326–E1332. [CrossRef]
28. Stegen, J.; Lin, X.; Konopka, A.; Fredrickson, J. Stochastic and deterministic assembly processes in subsurface microbial communities. *ISME J.* **2012**, *6*, 1653–1664. [CrossRef]
29. Liu, W.; Graham, E.; Dong, Y.; Zhong, L.; Zhang, J.; Qiu, C.; Chen, R.; Lin, X.; Feng, Y. Balanced stochastic versus deterministic assembly processes benefit diverse yet uneven ecosystem functions in representative agroecosystems. *Environ. Microbiol.* **2020**, *23*, 391–404. [CrossRef]
30. Tripathi, B.; Stegen, J.; Kim, M.; Dong, K.; Adams, J.; Lee, Y.K. Soil pH mediates the balance between stochastic and deterministic assembly of bacteria. *ISME J.* **2018**, *12*, 1072–1083. [CrossRef]
31. Zhang, K.; Shi, Y.; Cui, X.; Yue, P.; Li, K.; Liu, X.; Tripathi, B.; Chu, H. Salinity Is a Key Determinant for Soil Microbial Communities in a Desert Ecosystem. *mSystems* **2019**, *4*, e00225-18. [CrossRef] [PubMed]
32. Stegen, J.; Lin, X.; Fredrickson, J.; Chen, X.; Kennedy, D.; Murray, C.; Rockhold, M.; Konopka, A. Quantifying community assembly processes and identifying features that impose them. *ISME J.* **2013**, *7*, 2069–2079. [CrossRef] [PubMed]
33. Ning, D.; Deng, Y.; Tiedje, J.; Zhou, J. A general framework for quantitatively assessing ecological stochasticity. *Proc. Natl. Acad. Sci. USA* **2019**, *116*, 16892–16898. [CrossRef] [PubMed]
34. Meng, F. *Ralstonia solanacearum* Species Complex and Bacterial Wilt Disease. *J. Bacteriol. Parasitol.* **2013**, *4*, e119. [CrossRef]
35. Peng, J.; Liu, H.; Shen, M.; Chen, R.; Li, J.; Dong, Y. The inhibitory effects of different types of Brassica seed meals on the virulence of *Ralstonia solanacearum*. *Pest Manag. Sci.* **2021**, *77*, 5129–5138. [CrossRef]
36. Liu, H.; Dong, Y.H.; Shen, M.; Sun, F.; Wang, X.; Liu, J.; Li, J. Characteristics of Rhizosphere Microbial Communities in a Disease-suppressive Soil of Tomato Bacterial Wilt and its Disease-suppressive Transmission Mechanism. *Acta Pedol. Sin.* **2021**. [CrossRef]
37. Lu, R.K. *Analytical Methods of Soil and Agricultural Chemistry*; China Agricultural Science and Technology Press: Beijing, China, 1999.
38. Zhang, Z.; Liu, H.; Liu, X.; Chen, Y.; Lu, Y.; Shen, M.; Dang, K.; Zhao, Y.; Dong, Y.; Li, Q.; et al. Organic fertilizer enhances rice growth in severe saline-alkali soil by increasing soil bacterial diversity. *Soil Use Manag.* **2021**, *38*, 964–977. [CrossRef]
39. Schonfeld, J.; Heuer, H.; van Elsas, J.D.; Smalla, K. Specific and sensitive detection of Ralstonia solanacearum in soil on the basis of PCR amplification of fliC fragments. *Appl. Environ. Microb.* **2003**, *69*, 7248–7256. [CrossRef]
40. Caporaso, J.; Lauber, C.; Walters, W.; Berg-Lyons, D.; Lozupone, C.; Turnbaugh, P.; Fierer, N.; Knight, R. Global patterns of 16S rRNA diversity at a depth of millions of sequences per sample. *Proc. Natl. Acad. Sci. USA* **2011**, *108*, 4516–4522. [CrossRef]
41. Zhou, J.; Deng, Y.; Shen, L.; Wen, C.; Yan, Q.; Ning, D.; Qin, Y.; Xue, K.; Wu, L.; He, Z.; et al. Temperature mediates continental-scale diversity of microbes in forest soils. *Nat. Commun.* **2016**, *7*, 12083. [CrossRef]
42. Edgar, R. MUSCLE: Multiple Sequence Alignment with High Accuracy and High Throughput. *Nucleic Acids Res.* **2004**, *32*, 1792–1797. [CrossRef] [PubMed]
43. Quast, C.; Pruesse, E.; Yilmaz, P.; Gerken, J.; Schweer, T.; Yarza, P.; Peplies, J.; Glöckner, F. The SILVA ribosomal RNA gene database project: Improved data processing and web-based tools. *Nucleic Acids Res.* **2013**, *41*, D590–D596. [CrossRef] [PubMed]
44. Langille, M.G.; Zaneveld, J.; Caporaso, J.G.; McDonald, D.; Knights, D.; Reyes, J.A.; Clemente, J.C.; Burkepile, D.E.; Vega Thurber, R.L.; Knight, R.; et al. Predictive functional profiling of microbial communities using 16S rRNA marker gene sequences. *Nat. Biotechnol.* **2013**, *31*, 814–821. [CrossRef] [PubMed]
45. Deng, Y.; Jiang, Y.-H.; Yang, Y.; He, Z.; Luo, F.; Zhou, J. Molecular ecological network analyses. *BMC Bioinform.* **2012**, *13*, 113. [CrossRef] [PubMed]
46. Zhou, J.; Deng, Y.; Luo, F.; He, Z.; Tu, Q.; Zhi, X.Y. Functional Molecular Ecological Networks. *mBio* **2010**, *1*, e00169-10. [CrossRef] [PubMed]
47. Shannon, P.; Markiel, A.; Ozier, O.; Baliga, N.; Wang, J.; Ramage, D.; Amin, N.; Schwikowski, B.; Ideker, T. Cytoscape: A Software Environment for Integrated Models of Biomolecular Interaction Networks. *Genome Res.* **2003**, *13*, 2498–2504. [CrossRef]
48. Dalsing, B.; Allen, C. Nitrate Assimilation Contributes to Ralstonia solanacearum Root Attachment, Stem Colonization, and Virulence. *J. Bacteriol.* **2013**, *196*, 949–960. [CrossRef]
49. Yang, T.; Wei, Z.; Friman, V.P.; Xu, Y.; Shen, Q.; Kowalchuk, G.; Jousset, A. Resource availability modulates biodiversity-invasion relationships by altering competitive interactions. *Environ. Microbiol.* **2017**, *19*, 2984–2991. [CrossRef]
50. Xu, C.; Ding, W.; Li, S.; Liu, Y.; Wang, J.; Yang, L.; Zhang, S. Soil Acidification Aggravates the Occurrence of Bacterial Wilt in South China. *Front. Microbiol.* **2017**, *8*, 703. [CrossRef]
51. Dalsing, B.; Truchon, A.; Gonzalez-Orta, E.; Milling, A.; Allen, C. *Ralstonia solanacearum* Uses Inorganic Nitrogen Metabolism for Virulence, ATP Production, and Detoxification in the Oxygen-Limited Host Xylem Environment. *MBio* **2015**, *6*, e02471-14. [CrossRef]

52. Edwards, J.; Johnson, C.; Santos-Medellín, C.; Lurie, E.; Natarajkumar, P.; Bhatnagar, S.; Eisen, J.; Sundaresan, V. Structure, variation, and assembly of the root-associated microbiomes of rice. *Proc. Natl. Acad. Sci. USA* **2015**, *112*, E911–E920. [CrossRef] [PubMed]
53. Liu, Y.; Zhang, N.; Qiu, M.; Feng, H.; Vivanco, J.; Shen, Q.; Zhang, R. Enhanced rhizosphere colonization of beneficial Bacillus amyloliquefaciens SQR9 by pathogen infection. *FEMS Microbio. Lett.* **2014**, *353*, 49–56. [CrossRef] [PubMed]
54. Stringlis, I.; Yu, K.; Feussner, K.; de Jonge, R.; van Bentum, S.; Verk, M.; Berendsen, R.; Bakker, P.; Feussner, I.; Pieterse, C. MYB72-dependent coumarin exudation shapes root microbiome assembly to promote plant health. *Proc. Natl. Acad. Sci. USA* **2018**, *115*, E5213–E5222. [CrossRef] [PubMed]
55. Procópio, R.; Silva, I.; Martins, M.; Azevedo, J.; Araújo, J. Antibiotics produced by Streptomyces. *Braz. J. Infect. Dis. Off. Publ. Braz. Soc. Infect. Dis.* **2012**, *16*, 466–471. [CrossRef]
56. Nion, Y.A.; Toyota, K. Recent Trends in Control Methods for Bacterial Wilt Diseases Caused by *Ralstonia solanacearum*. *Microbes Environ.* **2015**, *30*, 1–11. [CrossRef]
57. Wei, Z.; Yang, X.; Yin, S.; Shen, Q.; Ran, W.; Xu, Y. Efficacy of Bacillus-fortified organic fertiliser in controlling bacterial wilt of tomato in the field. *Appl. Soil Ecol.* **2011**, *48*, 152–159. [CrossRef]
58. Laksmanan, V.; Selvaraj, G.; Bais, H. Functional Soil Microbiome: Belowground Solutions to an Aboveground Problem. *Plant Physiol.* **2014**, *166*, 689–700. [CrossRef]
59. Kéfi, S.; Berlow, E.L.; Wieters, E.A.; Navarrete, S.A.; Petchey, O.L.; Wood, S.A.; Boit, A.; Joppa, L.N.; Lafferty, K.D.; Williams, R.J. More than a meal ... integrating non-feeding interactions into food webs. *Ecol. Lett.* **2012**, *15*, 291–300. [CrossRef]
60. Thébault, E.; Fontaine, C. Stability of Ecological Communities and the Architecture of Mutualistic and Trophic Networks. *Science* **2010**, *329*, 853–856. [CrossRef]
61. Hu, J.; Wei, Z.; Friman, V.P.; Gu, S.H.; Wang, X.F.; Eisenhauer, N.; Yang, T.J.; Ma, J.; Shen, Q.R.; Xu, Y.C.; et al. Probiotic diversity enhances rhizosphere microbiome function and plant disease suppression. *mBio* **2016**, *7*, 8. [CrossRef]
62. Wu, J.; Barahona, M.; Tan, Y.J.; Deng, H.Z. Natural Connectivity of Complex Networks. *Chin. Phys. Lett.* **2010**, *7*, 295–298. [CrossRef]
63. Xiong, W.; Song, Y.; Yang, K.; Gu, Y.; Wei, Z.; Kowalchuk, G.; Xu, Y.; Jousset, A.; Shen, Q.; Geisen, S. Rhizosphere protists are key determinants of plant health. *Microbiome* **2020**, *8*, 27. [CrossRef] [PubMed]
64. Gao, M.; Xiong, C.; Gao, C.; Tsui, C.; Wang, M.; Zhou, X.; Zhang, A.; Cai, L. Disease-induced changes in plant microbiome assembly and functional adaptation. *Microbiome* **2021**, *9*, 187. [CrossRef] [PubMed]
65. Wei, Z.; Gu, Y.; Hu, J.; Yin, S.; Xu, Y.; Jousset, A.; Shen, Q.; Friman, V.P. *Ralstonia solanacearum* pathogen disrupts bacterial rhizosphere microbiome during an invasion. *Soil Biol. Biochem.* **2018**, *118*, 8–17. [CrossRef]
66. Nemergut, D.; Schmidt, S.; Fukami, T.; O'Neill, S.; Bilinski, T.; Stanish, L.; Knelman, J.; Darcy, J.; Lynch, R.; Wickey, P.; et al. Patterns and Processes of Microbial Community Assembly. *Microbiol. Mol. Biol. R.* **2013**, *77*, 342–356. [CrossRef]
67. Bahram, M.; Kohout, P.; Anslan, S.; Harend, H.; Abarenkov, K.; Tedersoo, L. Stochastic distribution of small soil eukaryotes resulting from high dispersal and drift in a local environment. *ISME J.* **2015**, *10*, 885–896. [CrossRef]
68. Jiao, S.; Lu, Y. Abundant fungi adapt to broader environmental gradients than rare fungi in agricultural fields. *Glob. Chang. Biol.* **2020**, *26*, 4506–4520. [CrossRef]